Nanoscale Res Lett (2009) 4:538–543
DOI 10.1007/s11671-009-9277-y

NANO EXPRESS

Multi-Stable Conductance States in Metallic Double-Walled Carbon Nanotubes

Dongsheng Tang · Yong Wang · Huajun Yuan · Lijie Ci · Weiya Zhou · Sishen Xie

Received: 2 December 2008 / Accepted: 9 February 2009 / Published online: 27 February 2009

Abstract Electrical transport properties of individual metallic double-walled carbon nanotubes (DWCNTs) were measured down to liquid helium temperature, and multi-stable conductance states were found in DWCNTs. At a certain temperature, DWCNTs can switch continuously between two or more electronic states, but below certain temperature, DWCNTs are stable only at one of them. The temperature for switching is always different from tube to tube, and even different from thermal cycle to cycle for the same tube. In addition to thermal activation, gate voltage scanning can also realize such switching among different electronic states. The multi-stable conductance states in metallic DWCNTs can be attributed to different Fermi level or occasional scattering centers induced by different configurations between their inner and outer tubes.

Keywords Carbon nanotube · Electrical transport property · Intertube interaction

Introduction

It is well established that the electrical properties of carbon nanotubes (CNTs) are sensitive to their nanostructures such as diameters, chiralities, defects, etc. [1–5]. In fact, CNTs prefer to be assembled as ropes by close-packing or as multi-walled CNTs (MWCNTs) by arranging them concentrically [6]. In both cases, interactions among nanotubes may significantly modify their electronic structures, and then introduce interesting variations in their electrical properties. For example, in the case of ropes of identical armchair single-walled CNTs (SWCNTs) intertube interactions can break their rotational symmetry, and then the π^* and π bands can mix, which will produce a pseudogap about 0.1 eV at the Fermi level [7–9]. As for MWCNTs, the case is a little more complicated because each one of these tubes has different diameters and can have different chiralities.

To explore the effect of the intertube interactions on electrical properties of MWCNTs, double-walled CNTs (DWCNTs) is the best candidate because they are the simplest MWCNTs to be dealt theoretically, which consist of only two tubes having the similar diameters as SWCNTs. In fact, most of the theoretical work on electronic structures of MWCNTs has been done based on DWCNTs [10–17]. Sanvito et al. [14] found that the interwall interactions may block some quantum conductance channels by investigating the electron transport properties of the commensurate DWCNTs. Roach et al. [15] inferred that the electronic propagation may follow a non-ballistic law based on the spreading properties of the wave packets in the incommensurate DWCNTs. Kwon and Tománek [16] found that the weak interwall interactions and changing symmetry can cause four pseudogaps to open and close periodically near the Fermi level during the soft librational motion. Recently, much experimental work has been specifically focused on this issue [17–21]. Kajiura et al. [17] demonstrated that the electrons pass through DWCNTs quasi-ballistically even at room temperature. Wang et al. [18] found that free charges in the inner metallic wall may screen the outer semiconducting wall from the gate effect. Moon et al. [20]

D. Tang (✉) · Y. Wang · H. Yuan
Key Laboratory of Low-Dimensional Quantum Structures and Quantum Control of Ministry of Education, College of Physics and Information Science, Hunan Normal University, Changsha 410081, China
e-mail: dstang@hunnu.edu.cn; dstang88@hotmail.com

L. Ci · W. Zhou · S. Xie
Institute of Physics, Chinese Academy of Sciences, Beijing 100080, China

determined the current-carrying capacity of each wall of DWCNTs by breaking down their wall sequentially under high bias voltages.

In this paper, we present electrical transport properties of individual metallic DWCNTs with highly transparent contacts. We found that conductance state of DWCNTs is multi-stable at low temperature. At a certain temperature, DWCNTs can switch between two or more electronic states, but below a certain temperature, DWCNTs is stable only at one of them. The temperature for switching is always different from tube to tube, and even different from thermal cycle to cycle for the same tube. In addition to thermal activation, gate voltage scanning can also realize such switching among different electronic states. This electrical behavior of DWCNTs is like the two level fluctuations or random telegraph signals observed in tunnel junctions, metal-oxide-semiconductor field-effect transistors (MOSFETs), and FETs based on *p*-type semiconducting SWCNTs. It can be attributed to different configurations or small movement between their inner and outer tubes under the equilibrium of the van der Waals interaction between layers with the elastic force of the graphene layers, which can affect the electronic structures of DWCNTs by shifting the Fermi level or inducing occasional electron scattering centers.

Experimental

DWCNTs used in our measurements were synthesized by pyrolizing C_2H_2 at a temperature of 900–1100 °C on floating iron catalysts promoted with sulfur. Diameters of outer tubes vary from 1.1 to 2.9 nm, and those of inner tubes from 0.4 to 2.2 nm, which was determined by transmission electron microscopy [22]. DWCNTs were first dispersed in an aqueous surfactant solution (1 wt% lithium dodecyl sulfate) and purified by centrifugation. Thereafter they were deposited on a highly *n*-doped silicon wafer with 100 nm SiO_2 layer by putting one droplet of suspension on the surface. Si wafer has been modified previously by amino-silanization. Electrodes were defined by using an electron beam lithography procedure with standard two-layer resist, and formed by evaporating 15 nm AuPd. Devices containing individual metallic DWCNTs with good source and drain contacts were selected for electrical transport measurements. The DWCNT between two electrodes is 150-nm long. The *n*-doped Si wafer was used as the back gate. The electrical transport measurements were carried out in a cryostat with a lock-in technique.

Results and Discussion

The most important feature of our DWCNT devices is that there are multi-stable conductance states at low temperature. As shown by the linear conductance versus temperature (*G*–*T*) curve of a metallic DWCNT (sample No. 1) (inset of Fig. 1), the linear conductance fluctuates unconventionally around 10 K, which looks like noises or fluctuations. However, they locate almost on the same level. By sweeping the bias voltage (V_D) continuously at around 10 K on this DWCNT immediately, we obtained four typical current versus V_D (I–V_D) curves, as indicated in Fig. 1. This indicates that this DWCNT seems to have different linear conductance for different V_D sweeping cycles under almost the same conditions (temperature fluctuations less than 0.05 K). It even can switch or fluctuate continuously between two levels in the same sweeping cycle, just like the two level fluctuations in tunnel junctions, MOSFETs, and FETs based on *p*-type semiconducting SWCNTs reported previously [23–25]. It seems that there are two electronic states in this DWCNT, and the DWCNT can stay stable at the low conductance state, the high conductance state, mixed state of them, and can even switch continuously between them. It also suggests that the mechanism for this kind of switching might be a slow process compared with the time scale of measurement.

As a matter of fact, the I–V_D curves are always non-linear. Figure 2 shows an I–V_D curve (inset) and the corresponding dI/dV–V_D curve (simultaneously recorded by the lock-in technique) of another metallic DWCNT (sample No. 2) in a large bias range. It indicates the same phenomenon as described above. Besides the difference in linear conductance around zero bias, another important feature of those two states is the difference in non-linearity indicated by the dI/dV–V_D curve. For the low conductance

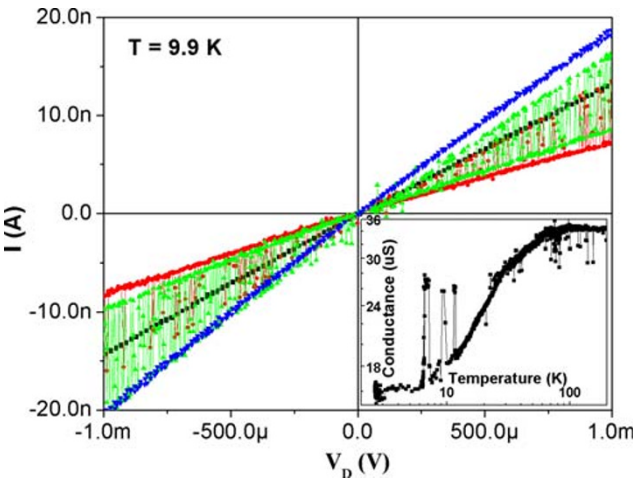

Fig. 1 Different I–V_D curves of a metallic DWCNT recorded around 9.9 K continuously indicate that there are multi-stable conductance states in this tube. Inset: Linear conductance of the DWCNT as a function of temperature from 300 to 2 K on a double logarithmic scale

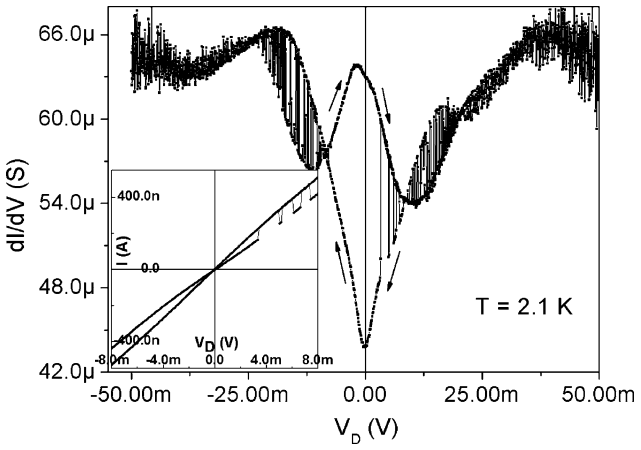

Fig. 2 The dI/dV–V_D and I–V_D (inset) curves recorded at the same time for another metallic DWCNT. The arrows indicate the sweeping directions

state, there is a dip; while for the high conductance state, there is a peak around zero bias. Furthermore, this dI/dV peak around zero bias does not respond to magnetic field as high as 10 Tesla.

Almost all our DWCNT samples exhibit sporadic changes in conductance, but only at a certain temperature, could the continuous switch between two or more levels be observed by careful measurements. After all, this kind of switching is sensitive to temperature, and can disappear even under temperature fluctuations less than 0.05 K. On the other hand, the temperature for conductance switching is different from tube to tube, even different from thermal cycle to cycle on the same tube. We have observed this kind of continuous switching on four different DWCNTs at 2.1, 4.9, 9.9, and even at 49.7 K, respectively.

In order to get more information about the different electronic states in DWCNTs, we have measured another metallic DWCNT (sample No. 3) very carefully. We recorded G–T curve when this DWCNT was cooled down, and dI/dV–V_D curves at different temperature when warmed up step by step. As shown in the inset of Fig. 3a, the conductance behaves completely different as temperature is cooled down in different thermal cycles: decreases in the first cooling process (black curve), but increases in the second one (after warming up from 2 to 130 K) and the third one (after warming up from 2 to 50 K) (red and green curves). Below 50 K, the G–T curves recorded in the second and third thermal cycles coincide with each other completely, which means that this tube is electrically stable during this measurement. Over 50–300 K, the G–T curves recorded in the first and second thermal cycles coincide with each other, and there is little change in conductance for both cases, which means that there is very low probability of electron–phonon scattering in this DWCNT, and the factor for the different conductance states in the

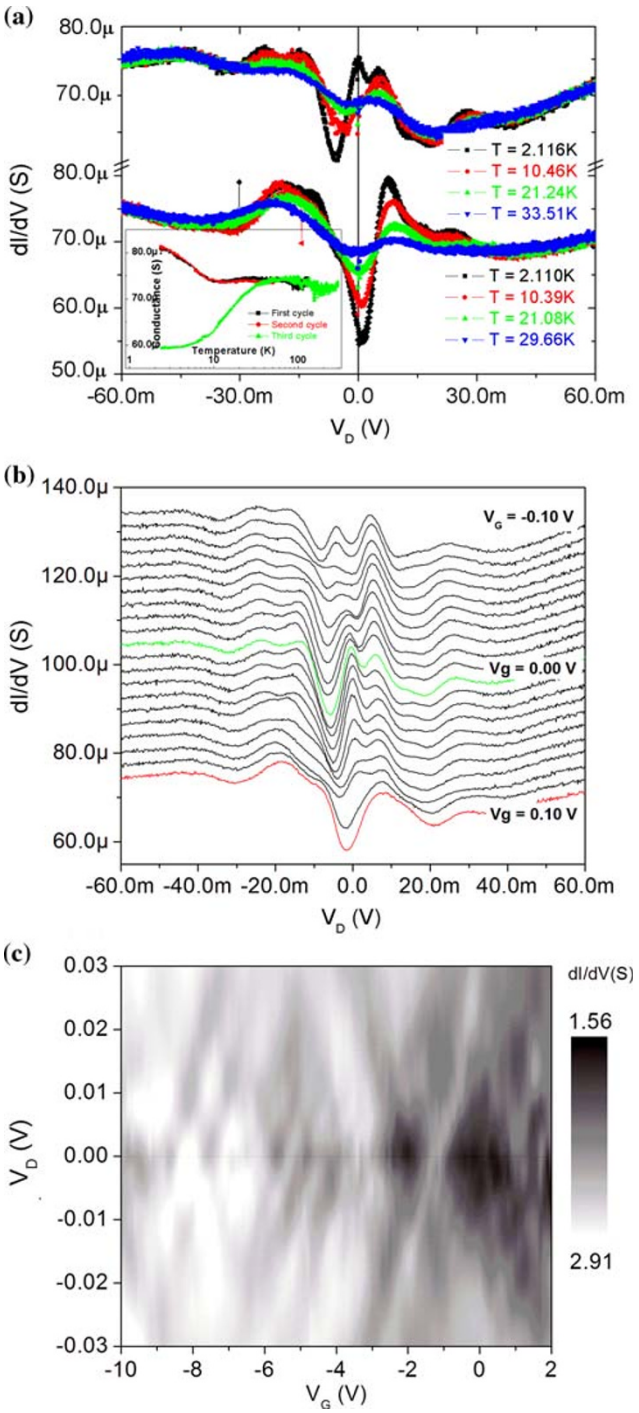

Fig. 3 **a** G–T curves of a metallic DWCNT recorded three times continuously when cooling down (Inset) and dI/dV–V_D curves recorded at various temperatures for the high conductance state (upside) and the low conductance state (downside) when heating up step by step. **b** The evolution of the dI/dV peaks around zero bias under small gate voltage (−0.1 to 0.1 V, step size: 0.01 V, curves shifted for clarity). **c** Two-dimensional dI/dV plot as a function of V_D and V_G

DWCNTs might be smeared by thermal activation. The corresponding dI/dV–V curves (Fig. 3a) indicate that around zero bias there is a peak for high conductance state

and a dip for low conductance state. As the temperature is lowered, the structures in dI/dV–V_D curve become sharper, i.e., the peak increases, while the dip decreases in conductance, but both saturate below 5 K, which is consistent with the G–T curves.

The evolution of the dI/dV peak around zero bias under small gate voltage (V_G) was shown in Fig. 3b, which indicates that this peak shifts and evolves into a dip with V_G. This process is completely reversible. In fact, the curve modulated by gate voltage ($V_G = 0.1$ V) is almost the same as the low conductance state curve in the downside of Fig. 3a, which indicates that V_G can realize switching between these two conductance states and may suggest different Fermi level positions for these two states. From the two-dimensional dI/dV plots (Fig. 3c, 5a) we can make a rough estimate of the capacitance between the DWCNT and the back gate: $C_G = 4e\ C/V$, where e is the charge of an electron. The excess charge Q on the DWCNT induced by V_G can be obtained as $Q = C_G V_G = 4e^*0.1 = 0.4e\ C$. Therefore, the different conductance states might be attributed to charges trapping in or escaping from impurities, defects on the DWCNT, or insulating layer adjacent to this tube.

As the case stands, our devices can be definitely switched to a relative high conductance state by positive V_G pulse (15 V), and a low conductance state by negative V_G pulse at high temperature (for example >72 K) (Fig. 4a). This is similar to the electrical hysteresis observed in semiconducting SWCNTs, and it is believed to be induced by the charges trapped in impurities or defects [26–28]. As the temperature is lowered, the electrical hysteresis weakens and fades away gradually, which means that the charges trapped in impurities or defects become fewer and fewer. When the temperature is lower than 72 K, the DWCNT becomes electrically unstable after V_G sweeping, and the change in conductance is random and unpredictable. Furthermore, the lower the temperature is, the larger the change in conductance is. That is to say, at low temperature, the V_G pulse cannot change the electronic state directly by trapping charges in impurities or defects. However, it disturbs the electronic state of DWCNTs in its own way. Figure 4b shows all kind of dI/dV–V_D curves recorded repeatedly on the DWCNT after being disturbed by a positive V_G pulse at 2.280 K. It indicates that this DWCNT switches among different electronic states indeed. Around zero bias, there can be a peak or a dip corresponding to different electronic states just as shown in Fig. 2.

Our individual metallic DWCNT devices have good source and drain contacts. They are much different from the tunnel junctions and MOSFETs that exhibit two level conductance fluctuations [23, 24], and also different from the semiconducting SWCNT-based FETs that exhibit random telegraph noise at high temperature (200 K, for example) and stable electrical hysteresis at low temperature

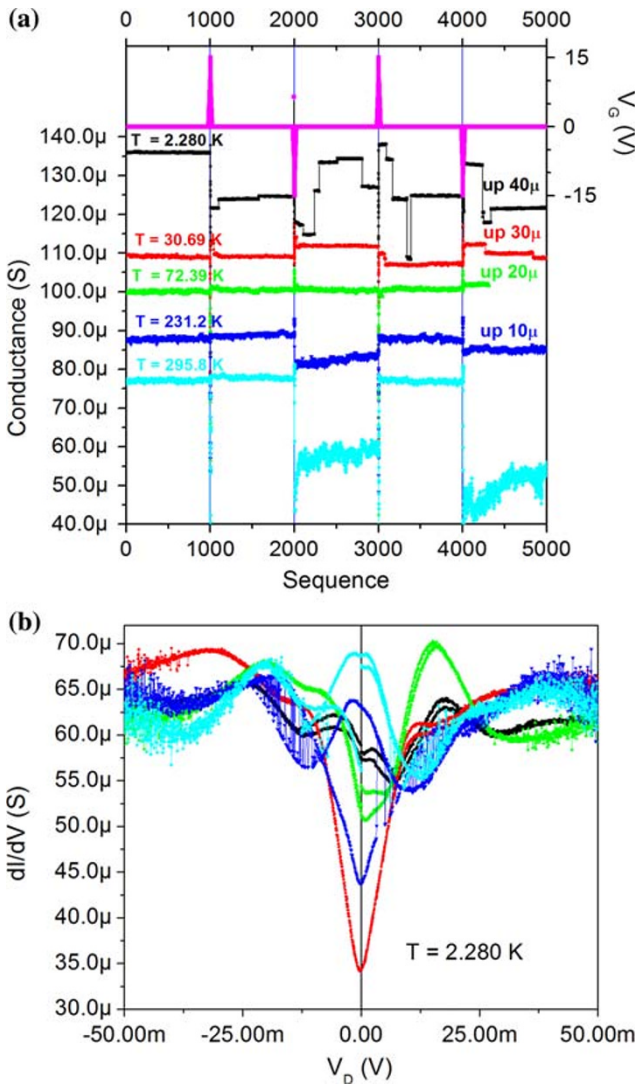

Fig. 4 **a** Linear conductance of a metallic DWCNT (sample No. 2) as a function of time, recorded under periodic V_G pulse at different temperature (curves shifted for clarity), which shows that the DWCNT exhibits electrical hysteresis behavior at high temperature (>72.39 K) and is electrically unstable at low temperature (<72.39 K). **b** The dI/dV curves of the DWCNT recorded repeatedly after being disturbed by a positive V_G pulse (15 V) at 2.280 K in another thermal cycle

(5 K) [24, 28]. After all the non-localized electrons transport ballistically through the tubes (to be discussed later), the density of impurities or defects in our DWCNTs is very low. Other than charges trapped in impurities or defects, there might be a new mechanism that bring on the multistable electronic states, and can be disturbed by the V_G and thermal activation.

The two-dimensional dI/dV plot as a function of V_D and V_G for the sample No. 3 (Fig. 3c) indicates that the positions of the dI/dV dips and peaks evolve smoothly and periodically pointing to a Fabry–Perot interference pattern, which means that the peaks and dips of dI/dV curve come

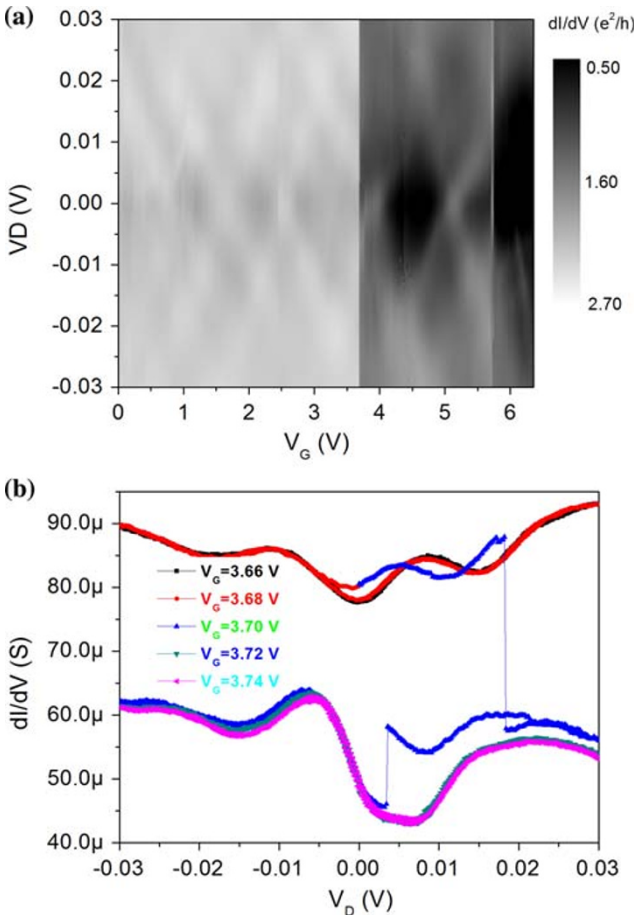

Fig. 5 **a** Two-dimensional *dI/dV* plot as a function of V_D and V_G measured at 5.0 K for a metallic DWCNT. **b** The *dI/dV*–V_D curves around the distinct boundary of the two-dimensional *dI/dV* plot as shown in (**a**)

from quantum interference between the propagating electron waves [29]. On the other hand, this pattern is somewhat irregular, having different periodicities in different parts and being asymmetric with V_D, which points to a non-ideal Fabry–Perot interference pattern due to minor disorder or inhomogeneity along this tube. Figure 5a shows a two-dimensional *dI/dV* plot as a function of V_D and V_G for another DWCNT (sample No. 4, $d = 2.5$ nm and $L = 150$ nm). It consists of two patterns with distinct boundary at $V_G = 3.70$ V. On the left side, the regular interference pattern means a perfect Fabry–Perot resonator with an interference peak at $V_D = V_C = h\upsilon_F/2eL = 11.1$ mV ($\upsilon_F = 8.1 \times 10^5$ m/s is the Fermi velocity and $L = 150$ nm is the length of tube). It indicates that electron scattering occurs mostly at the nanotube–electrode interface and electrons pass through the nanotube ballistically. On the other hand, firstly the conductance decreases suddenly overall (also see Fig. 5b); secondly the V_D and V_G spacing between adjacent peaks (dips) increases (about two times); thirdly the *dI/dV* curves become asymmetric. All of these point to a fact that there is a disorder which serves as a new electron-backscattering center ($V'_D = V'_C = h\upsilon_F/2eL' = 22.2$ mV, then $L' = 75$ nm) appearing in the middle of the tube, and that the tube has been hole doped by the new mechanism. When measured in another thermal cycle, this kind of electron-backscattering center disappeared, and regular Fabry–Perot interference pattern will appear again in all the V_G sweeping range (0–20 V). It means that the appearance or disappearance of this kind of electron-backscattering center is reversible, and V_G is not the sufficient condition to activate this kind of disorder, and that there is no or few impurities or defects in our DWCNTs. This kind of disorder can be observed again, but only by chance. By carefully checking Fig. 5b, we found out that the abrupt change in *dI/dV* consists of two parts: decrease in the overall conductance and *dI/dV* peaks shifting versus V_D. The former might be due to the appearance of electron scattering center, and the latter might be due to the shift of Fermi level induced by charge accumulation. In our measurements on DWCNTs, these two kinds of change have been observed independently or synchronously.

The electrical transport properties of DWCNTs characterized by multi-stable conductance states might originate from their larruping microstructures: small diameter and two layers. It is said that the weak interwall interactions can activate low-frequency librational motion about and vibration motion normal to the tube axis for the inner tube in DWCNTs [16]. It may be hard to believe that the entire inner tube vibrate or librate; however, it is possible for some small part of the twisted inner tube to vibrate or librate independently under the equilibrium of the van der Waals interaction between layers with the elastic force of the graphene layers. There may be orientational dislocations or twist frozen in DWCNTs during their synthesis. High resolution transmission electron microscopy (HR-TEM) observation revealed that there are smaller (0.39 nm) interlayer spaces with the commensurate lattice and larger (0.54 nm) spaces also in the same DWCNT [30]. Calculations also indicated that the interwall interactions can induce electron transfer from outer tube to interwall region, and then the outer tube can be viewed as being hole doped by the inner tube [31]. When the inner tube (or part of it) changes its configuration about the tube axis sporadically, the amount of charge transfer will change accordingly, and then the Fermi level will shift. We believe that the V_G can disturb the charge distribution in the interwall region, and then the configuration of DWCNTs. When the inner tube vibrates normal to the tube axis, the inner tube is close to the outer tube on one side and far away on the other side, which will serve as the new factor for electron scattering [32].

Therefore, we consider that the multi-stable conductance states in DWCNTs can be attributed to the different

configurations of its outer and inner tubes. The continuously switching between two electronic states can be attributed to the locally orientational depinning or melting of a small part of inner tube at certain temperature (T_{OM}, 9.9 K for sample No. 1). When the temperature is lower than T_{OM}, the two tubes are pinned and the vibration of inner tube is small, and then the DWCNT is electronically stable at different states due to the different configurations. At relatively high temperature ($>T_{OM}$) one or more parts of inner tube can vibrate freely and independently. All states from different configurations can contribute to the electrical properties at the same time, and then the DWCNT is also stable at a mixed state. When just at T_{OM}, one part of the inner tube can switch continuously and slowly under the equilibrium of the van der Waals interaction between layers with the elastic force of the graphene layers, and so does the conductance. Because the orientational disorder is different from tube to tube, even different from thermal cycle to cycle on the same tube; the temperature for orientational melting T_{OM} is also different from tube to tube.

Conclusions

We have observed multi-stable conductance states in DWCNTs at liquid helium temperature. At a certain temperature, DWCNTs can switch continuously between two or even more electronic states. Below certain temperature, DWCNTs can be stable at different electronic states due to different Fermi level or occasional scattering centers induced by different configurations between their inner and outer tubes. The temperature for switching is always different from tube to tube, and even different from thermal cycle to cycle for the same tube. This electrical behavior might shed light on the effect of inter-walled interactions on the electrical transport properties of MWCNTs.

Acknowledgments This work was supported by the Major Research plan of National Natural Science Foundation of China (Grant No. 90606010), the Program for New Century Excellent Talents in University (Grant No. NCET-07-0278) and the Hunan Provincial Natural Science Fund of China (Grant No. 08JJ1001).

References

1. N. Hamada, S.I. Sawada, A. Oshiyama, Phys. Rev. Lett. **68**, 1579 (1992). doi:10.1103/PhysRevLett.68.1579
2. C.T. White, T.N. Todorov, Nature **393**, 240 (1998). doi:10.1038/30420
3. C.L. Kane, E.J. Mele, Phys. Rev. Lett. **78**, 1932 (1997). doi:10.1103/PhysRevLett.78.1932
4. S.J. Tans, A.R.M. Verschueren, C. Dekker, Nature **393**, 49 (1998). doi:10.1038/29954
5. M.K. Ge, K. Sattler, Science **260**, 515 (1993). doi:10.1126/science.260.5107.515
6. A. Thess, R. Lee, P. Nikolave, H. Dai, P. Petit, J. Robert, C. Xu, Y.H. Lee, S.G. Kim, A.G. Rinzler, D.T. Colbert, G.E. Scuseria, D. Tománek, J.E. Fisher, R.E. Smalley, Science **273**, 483 (1996). doi:10.1126/science.273.5274.483
7. P. Delaney, H.J. Choi, J. Ihm, S.G. Louie, M.L. Cohen, Nature **391**, 466 (1998). doi:10.1038/35099
8. Y.K. Kwon, S. Saito, D. Tománek, Phys. Rev. B **58**, R13314 (1998). doi:10.1103/PhysRevB.58.R13314
9. M. Ouyang, J.L. Huang, C.L. Cheung, C.M. Lieber, Science **292**, 702 (2001). doi:10.1126/science.1058853
10. L. Langer, V. Bayot, E. Grivei, J.P. Issi, J.P. Heremans, C.H. Olk, L. Stockman, C. Van Haesendonck, Y. Bruynseraede, Phys. Rev. Lett. **76**, 479 (1996). doi:10.1103/PhysRevLett.76.479
11. A. Bachtold, C. Strunk, J.P. Salvetat, J.M. Bonard, L. Forró, T. Nussbaumer, Nature **397**, 673 (1999). doi:10.1038/17755
12. C. Schönenberger, A. Bachtold, C. Strunk, J.P. Salvetat, L. Forró, Appl. Phys. A **69**, 283 (1999)
13. A. Latgé, D. Grimm, Carbon **45**, 1905 (2007). doi:10.1016/j.carbon.2007.04.019
14. S. Sanvito, Y.K. Kwon, D. Tománek, C.J. Lambert, Phys. Rev. Lett. **84**, 1974 (2000). doi:10.1103/PhysRevLett.84.1974
15. S. Roche, F. Triozon, A. Rubio, D. Mayou, Phys. Rev. B **64**, 121401-1 (2001). doi:10.1103/PhysRevB.64.121401
16. Y.K. Kwon, D. Tománek, Phys. Rev. B **58**, R16001 (1998). doi:10.1103/PhysRevB.58.R16001
17. H. Kajiura, H. Huang, A. Bezryadin, Chem. Phys. Lett. **398**, 476 (2004). doi:10.1016/j.cplett.2004.09.115
18. S. Wang, X.L. Liang, Q. Chen, Z.Y. Zhang, L.M. Peng, J. Phys. Chem. B **109**, 17361 (2005). doi:10.1021/jp053739+
19. D.S. Tang, L.J. Ci, W.Y. Zhou, S.S. Xie, Carbon **44**, 2155 (2006). doi:10.1016/j.carbon.2006.03.023
20. S. Moon, W. Song, N. Kim, J. Sung Lee, P.S. Na, S.G. Lee, J. Park, M.H. Jung, H.W. Lee, K. Kang, C.J. Lee, J. Kim, Nanotechnology **18**, 235201 (2007). doi:10.1088/0957-4484/18/23/235201
21. I. Maeng, C. Kang, S.J. Oh, J.H. Son, K.H. An, Y.H. Lee, Appl. Phys. Lett. **90**, 051914 (2007). doi:10.1063/1.2435338
22. L.J. Ci, Z.L. Rao, Z.P. Zhou, D.S. Tang, X.Q. Yan, Y.X. Liang, D.F. Liu, H.J. Yuan, W.Y. Zhou, G. Wang, W. Liu, S.S. Xie, Chem. Phys. Lett. **359**, 63 (2002). doi:10.1016/S0009-2614(02)00600-0
23. X. Jiang, M.A. Dubson, J.C. Garland, Phys. Rev. B **42**, 5427 (1990). doi:10.1103/PhysRevB.42.5427
24. K.R. Farmer, C.T. Rogers, R.A. Buhrman, Phys. Rev. Lett. **58**, 2255 (1987). doi:10.1103/PhysRevLett.58.2255
25. F. Liu, M.Q. Bao, H.J. Kim, K.L. Wang, C. Li, X.L. Xiao, C.W. Zhou, Appl. Phys. Lett. **86**, 163102-1 (2005). doi:10.1063/1.1901822
26. J.B. Cui, R. Sordan, M. Burghard, K. Kern, Appl. Phys. Lett. **81**, 3260 (2002). doi:10.1063/1.1516633
27. W. Kim, A. Javey, O. Vermesh, Q. Wang, Y. Li, H. Dai, Nano. Lett. **3**, 193 (2003). doi:10.1021/nl0259232
28. B.M. Kim, Y.F. Chen, M.S. Fuhrer, Fullerenes **12**, 541 (2002)
29. W. Liang, M. Bockrath, D. Bozovic, J.H. Hafner, M. Tinkham, H. Park, Nature **411**, 665 (2001). doi:10.1038/35079517
30. A. Hashimoto, K. Suenaga, K. Urita, T. Shimada, T. Sugai, S. Bandow, H. Shinohara, S. Iijima, Phys. Rev. Lett. **94**, 045504-1 (2005). doi:10.1103/PhysRevLett.94.045504
31. Y. Miyamoto, S. Saito, D. Tománek, Phys. Rev. B **65**, 041402-1 (2001). doi:10.1103/PhysRevB.65.041402
32. D. Orlikowski, H. Mehrez, J. Taylor, H. Guo, J. Wang, C. Roland, Phys. Rev. B **63**, 155412-1 (2001). doi:10.1103/PhysRevB.63.155412